INTERNATIONAL
Agrophysics
www.international-agrophysics.org

Int. Agrophys., 2022, 36, 257-267
doi: 10.31545/intagr/152488

Investigation of mechanical properties of cotton stalk based on multi-component analyses**

Weisong Zhao[1,2], *Jianhua Xie*[1]*, *Zhenwei Wang*[2], *Qiming Gao*[2], *and Mingjiang Chen*[2]

[1]College of Mechanical and Electrical Engineering, Xinjiang Agricultural University, Urumqi 830052, China
[2]Biomass Conversion and Utilization Equipment Innovative Research Group of Science and Technology Innovative Engineering of the Chinese Academy of Agricultural Science, Nanjing Institute of Agricultural Mechanization, Ministry of Agriculture and Rural Affairs, Nanjing 210014, China

Received January 4, 2022; accepted July 28, 2022

A b s t r a c t. A comprehensive understanding of the uprooting failure mechanism will likely require the accurate characterization of the mechanical properties of cotton stalk. Uprooting failure includes a fractured cotton stalk and peeled phloem sliding along the xylem. The modulus of elasticity of cotton stalk and its tissues (xylem and phloem) were measured using three different modes (tensile, compression and bending), and the reasons for the fractured cotton stalk and the peeled phloem sliding along the xylem were analysed from the perspective of composite mechanics. The results showed that the cotton stalk radially conforms to the properties of the composite with transverse anisotropy. The axial modulus of elasticity was significantly larger than the radial modulus of elasticity (axial modulus of elasticity: cotton stalk is 3181.79 MPa, xylem is 1093.91 MPa, phloem is 249.89 MPa, radial modulus of elasticity: is 91.04 MPa, xylem is 83.77 MPa, phloem is 77.01 MPa). Xylem is the backbone of the stalk that provides 96% of its compressive strength. The direct cause of fractured cotton stalk originated from the load force that exceeded its intrinsic compressive strength. Peeled phloem sliding along the xylem was related for the most part to the different radial modulus of elasticity of the xylem and phloem, and the weak cohesion between these two tissues. Based on the results, some suggestions were provided for the design of a puller.

K e y w o r d s: cotton stalk, elastic modulus, composite material, uprooting

*Corresponding author e-mail: xjh199032@163.com
**This work was supported by the National Natural Science Foundation of China (Grant No. 51505242, 2016-2018), the Agricultural Science and Technology Innovation Programme of the Chinese Academy of Agricultural Sciences (ASTIP, CAAS), Project Plan of Science and Technology Supporting Xinjiang in Autonomous Region (Grant No. 2021E02005, 2021-2023), and Tianshan Innovation Team Project (Grant No. 2020D14037, 2020-2023).

INTRODUCTION

Cotton stalk is the primary by-product of cotton production, and is rich in cellulose, lignin, and crude protein (Li *et al*., 2018), it is an important supplement to resource utilization in the form of biochar (Chen X. *et al*., 2015; Hou *et al*., 2014; Hu *et al*., 2014). According to the China Statistical Yearbook, in 2019, the sown area of cotton in China was 3.3392×10^6 ha, and the total yield was 5.889×10^6 t, of which Xinjiang accounted for 76.08% of the total and is therefore the main cotton plantation area in China.

Uprooting and harvesting are the most important aspects of realizing the utilization of cotton stalk but they are also the weakest link in this process. In order to efficiently collect whole cotton stalks in Xinjiang, a large number of studies concerning the optimum design of the stalk uprooting mechanism have been carried out (Zhao *et al*., 2019; Cai *et al*., 2020; Chen *et al*., 2019a; He *et al*., 2020; Tang *et al*., 2010). However, cotton stalks are short and thin, which involves serious challenges in the uprooting process for high-density planting (Wu *et al*., 2015). A large number of whole or broken cotton stalks remained in the cotton field after the operation of the stalk-uprooting machine (failure of uprooting), and the stalk-removing ratio proved to be inadequate. As shown in Fig. 1, in one case, the so-called fractured cotton stalk (FCS): the cotton stalk fractured at the holding position and the lower part

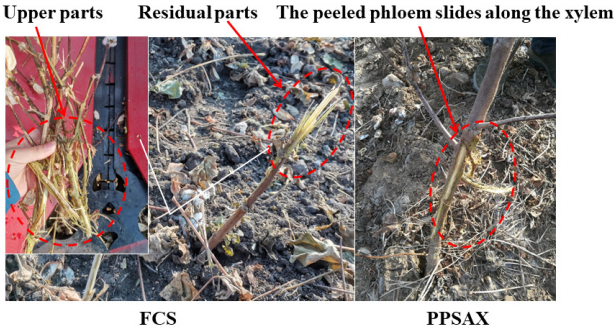

Fig. 1. States of the cotton-stalk uprooting failure.

was left in the field; in the other case, the peeled phloem slides along the xylem (PPSAX) which is one of the most important reasons causing the failure of the cotton stalk to be pulled out. The two scenarios of FCS and PPSAX are the common manifestations of cotton stalk uprooting failure. In the process of the mechanized uprooting of cotton stalk, the impacts of the weather, nutrients and other environmental factors, the diameter and the moisture content of the cotton stalk were quite different, leading to a large gradient range in the mechanical properties of the cotton stalk, and further affecting the failure of the uprooting ratio.

In order to address this problem, some researchers have studied the structural design and optimization (Ramadan *et al*., 2010; Chen *et al*., 2019b; Zhang *et al*., 2021), some researchers have focused on the experimental analysis of the mechanical properties of the cotton stalk (Jha *et al*., 2008; Zhang *et al*., 2014; Chen M. *et al*., 2015; Li *et al*., 2011) which forms the basis of the design of agricultural processing machinery such as those for uprooting, crushing, and harvesting. The current research included the influence of moisture content, sampling position, and sampling time on the mechanical properties of the stalk (Aydın and Arslan 2018; Liang *et al*., 2020; Shi *et al*., 2017). At present, there is insufficient research concerning the mechanism of the phloem sliding along the xylem and breaking the cotton stalk from the viewpoint of the mechanical properties of the cotton stalk. A study concerning the mechanism of FCS and MCS would contribute to the exploration of the relationship between the properties of the cotton stalk and the mechanism of uprooting, and further improve the quality and efficiency of cotton stalk-uprooting equipment.

As mentioned above, uprooting fracture is a serious challenge in the harvesting of cotton stalk. Developing a sufficient degree of understanding concerning the compression of FCS and PPSAX will most likely require the accurate characterization of the mechanical properties of cotton stalk. One of the most important mechanical properties for structural analysis is the various elastic parameters. The purpose of this study was to measure the elastic parameters of the cotton stalk and their tissues using three different loading modes (tensile, compression and three-point bending), and to attempt to understand the cause of FCS and PPSAX based on a mechanical properties analysis. Ultimately, the results may provide a guide for improving the design of uprooting machinery.

MATERIALS AND METHODS

Xinluzao 64, which is one of the cotton varieties grown in Xinjiang, was used as the test material and was sampled from a research field at Xinjiang Uygur Autonomous Region Academy of Agricultural Sciences on September 28, 2020. The planting pattern was a mulching pattern with a wide row (inter-row) spacing of 660 mm and a narrow row (intra-row) spacing of 100 mm, as shown in Fig. 2. The planting density was 19 000 plants ac^{-1}. The stalk growth was normal, satisfactory, and straight without apparent defects.

Theoretically, the lower the clamping position, the better the stalk removal effect when pulling up cotton stalks. However, due to the size limitation of the mechanical structure, the clamping position is usually 10-30 cm above the soil (Fig. 3). Therefore, one hundred cotton stalks were collected from this position. First, the xylem and phloem were manually peeled. Then, the stalks and their components (xylem and phloem) were cut according to the requirements of the tests (tensile, compression and bending), with the specific dimensions described below. Only stalks that were found to be free of pests and disease damage were included in the study. In the end, 80 test samples were obtained.

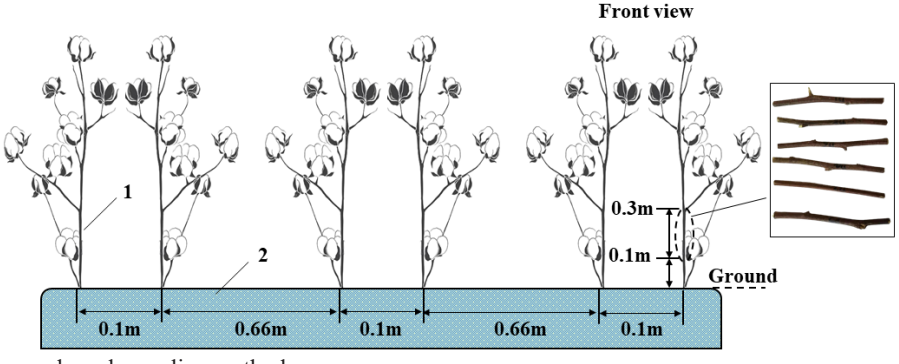

Fig. 2. Close planting mode and sampling method.

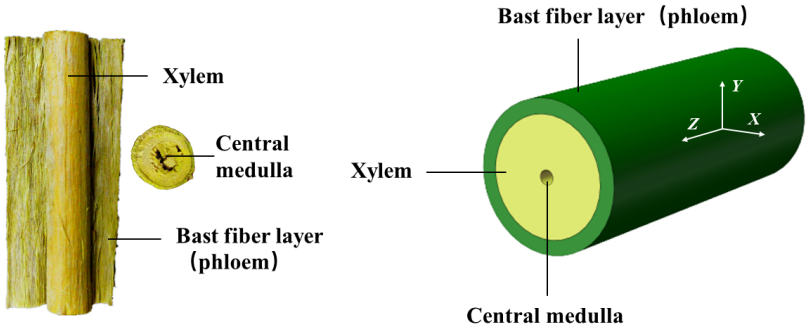

a. Diagram of cotton stalk b. Geometrical model of cotton stalk

Fig. 3. Structural composition and geometrical model of the cotton stalk.

To more realistically reflect the mechanical state of the cotton stalks during the stalk puller operation, cotton stalks were collected during the normal time period of stalk puller operation (September 28, 2020). The cotton stalk moisture content was maintained in its natural state from its time in the field. The average value of the cotton stalk moisture content was 66.4%. Tests were carried out immediately after the samples were taken, and all of the mechanical measurements were performed in a laboratory setting using the same universal testing device (UTM6503, developed by Shenzhen Sansi Zongheng Technology Co., Ltd.).

Axial tensile and radial compression tests were performed on the stalk, xylem and phloem, with 10 repetitions of each set of tests, for a total of 60 tests. The three-point bending tests were performed on the stalk and xylem, with 10 repetitions for each group, making a total of 20 tests. The total number of tests performed overall was 80. The data from each group of 10 test repetitions were processed by removing the maximum and minimum values to reduce test errors. The means ± standard deviation (Sd.) were calculated using the same variables. The test values of the rupture force and the modulus of elasticity in two directions for the stalk, xylem and phloem were obtained using the aforementioned tests. The phloem could not be tested for three-point bending, but its bending modulus could be obtained through the derivation of the formula above. After obtaining the required data, the test values of the modulus of elasticity of the stalks were compared with the calculated values under the assumptions of the composite model, which was used to verify the correctness of the assumption of the presence of transverse orthogonal anisotropic material within the cotton stalks.

The cotton stalk belongs to the annual Gramineae family of monocotyledonous flowering plants, and has roots, a stalk, and crown. The root contains the highest percentage of lignin from among the three parts and has the strongest mechanical properties. The cross section of the cotton stalk in this area consists of the pith, xylem, and phloem, and may be approximated by a circle (Fig. 3a). The material, diameter, and wall thickness of each component were also assumed to be uniform. The coordinate axis, the z-axis of the stem, and also the radial x- and y-axes were established as shown in Fig. 3b.

The properties of cotton stalk may be characterized using nine engineering elastic parameters: axial elastic modulus E_Z, radial elastic moduli E_X and E_Y; connatural-plane axial shear modulus G_{XY}, and anisotropic-plane axial shear moduli G_{YZ} and G_{XZ}; connatural-plane Poisson's ratio μ_{XY} and anisotropic-plane Poisson's ratios μ_{YZ} and μ_{XZ}. According to its assumed shape, the axial section of the cotton stalk is distributed with a symmetry radiating from a central point, *i.e.*, it is a cross-sectional anisotropy material. Therefore, its engineering elastic parameters meet Eq. (1) (Shen *et al.*, 2015):

$$\begin{cases} E_X = E_Y \\ G_{YZ} = G_{XZ} \\ \mu_{YZ} = \mu_{XZ} \\ G_{XY} = \dfrac{E_X}{2(1+\mu_{XY})} \end{cases}, \tag{1}$$

where: E_X and E_Y are the radial elasticity modulus (MPa), G_{XY} is the connatural-plane axial shear modulus (MPa), G_{YZ}, G_{XZ} are anisotropic-plane axial shear modulus (MPa), μ_{XY} is the connatural-plane Poisson's ratio, μ_{YZ} and μ_{XZ} are anisotropic-plane Poisson's ratio.

Cotton stalks have tapered structures with diameter changes along their length. In order to reduce the error, the diameter of the sample was calculated as the equivalent diameter D_e, as shown in Eq. (2):

$$\begin{cases} D_e = \dfrac{D_{max} + D_{min}}{2} \\ V_M = \dfrac{(D_e - 2h)^2 - D_i^2}{D_e^2 - D_i^2} \\ V_R = 1 - V_M \end{cases}, \tag{2}$$

where: D_{max} is the maximum diameter, D_{min} is the minimum diameter, D_i is the core diameter, and h is phloem thickness, respectively. Their mean values were obtained (D_e = 7.08 mm, D_i = 0.76 mm, h = 0.80 mm) by measuring 10 samples. According to Eq. (2), the xylem-stalk and phloem-stalk volume ratios were 59.4 and 40.6%, respectively.

The elasticity modulus E may be calculated from the stress and strain (Eq. (3)) of the linear segment of the curve after fitting. The xylem, phloem, and cotton stalk were all subjected to an axial tension test in order to obtain their axial tensile elasticity moduli E_{Z2}, E_{Z3}, and E_{Z1}, respectively. Meanwhile, the axial tensile elasticity moduli of the various tissues were tested using the relational expression of the composite material engineering constant as follows:

$$\begin{cases} E=\dfrac{\sigma}{\varepsilon} \\ E_{Z1}=E_{Z2}V_M+E_{Z3}V_R\,, \end{cases} \tag{3}$$

where: E is the elasticity modulus (MPa), σ is the stress (MPa), ε is the strain, and E_{Z1}, E_{Z2}, and E_{Z3} are the axial tensile elasticity moduli of the cotton stalk, xylem, and phloem (MPa), respectively.

The tissues were subjected to a radial compressive test in order to obtain their respective compressive elasticity moduli E_{X2}, E_{X3}, and E_{X1}. The moduli were evaluated using the relational expression of the composite material engineering constant (Eq. (4)).

$$E_{X1}=\frac{E_{X2}E_{X3}}{V_M E_{X3}+V_R E_{X2}}, \tag{4}$$

where: E_{X1}, E_{X2}, and E_{X3} are the radial compressive elasticity moduli of the cotton stalk, xylem, and phloem (MPa).

The radial shear stiffness U_{YZ2} and U_{YZ2} and the bending shear moduli G_{YZ2} and G_{YZ1} of the tissues were obtained by referring to the equations of circular tube shear stiffness Eq. (5)) and modulus (Eq. (6)) in the Test Method for Flexural Properties of Sandwich Constructions (GB1456-2005):

$$U=\frac{\Delta F L_s}{4\left(f-\dfrac{f_1 L_s}{3a}\right)}, \tag{5}$$

where: U is the shear stiffness (N), ΔF represents the load increment of the elastic stage (N), L_s denotes the span (mm), f indicates the mid-span deflection increment (mm), f_1 denotes the epitaxial deflection increment (mm), and a is the extrapolation length (mm) (GB1456-2005):

$$G=\frac{2U}{\pi/4(D_e^2-D_i^2)}=2.548\frac{U}{D_e^2-D_i^2}\,, \tag{6}$$

where: G is the bending shear modulus (MPa).

The bending shear moduli G_{YZ2} and G_{YZ1} of the xylem and cotton stalk were calculated using Eq. (6). As the phloem could not be subjected to a three-point bending test, its bending shear modulus must be calculated theoretically. G_{YZ3} of the phloem may be derived from the relational expression of the composite material engineering constant, as follows:

$$G_{YZ1}=\frac{G_{YZ2}G_{YZ3}}{V_M G_{YZ2}+V_R G_{YZ3}} \Leftrightarrow G_{YZ3}=\frac{V_M G_{YZ1}G_{YZ2}}{G_{YZ2}-V_R G_{YZ1}}, \tag{7}$$

where: G_{YZ2} and G_{YZ1} are the bending shear moduli of the xylem and stalk (MPa), respectively, and G_{YZ3} is the bending shear modulus of the phloem (MPa).

The axial torsional shear modulus could not be measured directly; therefore, the connatural-plane Poisson's ratios μ_{XY2} and μ_{XY1} of the xylem and cotton stalk were assumed to be 0.6, and μ_{XY3} of the phloem was assumed to be 0.3 by referring to Poisson's ratio of similar materials and combined with the equations from the following studies (Tan *et al*., 2020; Wang *et al*., 2017). Thus, the axial torsional shear modulus G_{XY} was calculated from Eq. (1).

The parameter relationship (Eq. (8)) of the orthogonal anisotropic material was derived according to the mechanics of composite materials. Meanwhile, the anisotropic-plane Poisson's ratio μ_{YZ} was derived from the values of the radial compressive elasticity modulus E_X, axial tensile elasticity modulus E_Z, and the connatural-plane Poisson's ratio μ_{XY}:

$$\mu_{YZ}<\frac{1}{\sqrt{2\mu_{XY}}}\frac{E_X}{E_Z}, \tag{8}$$

where: μ_{YZ} is the anisotropic-plane Poisson's ratio and μ_{XY} is the connatural-plane Poisson's ratio.

The axial tensile (Z-axis direction in Fig. 3b) tests of cotton stalks and its tissues were carried out. The xylem and cotton stalk were cut into samples with lengths of 120 mm and equivalent diameters of 6-8 mm, the phloem was cut into samples with lengths of 80 mm and widths of 6 mm. The thickness remained changed, and this parameter depended upon the materials itself. A pretension force of <5 N was initiated. The samples were loaded at a velocity of 5 mm min^{-1} in the axial direction. The elastic moduli of various tensile parameters were obtained by substituting the latter in Eq. (3).

The xylem and cotton stalk were cut into samples with lengths of 20 mm and equivalent diameters of 6-8 mm, with an unchanged material thickness. The phloem was cut into a square sample with dimensions of 20 × 20 mm with an unchanged thickness. A pretension force of <5 N was applied on the samples using a squeezing block at a loading velocity of 5 mm min^{-1} in a radial direction.

Based on a standard method (American Society of Agricultural Engineers, 2017), the moduli of elasticity of the xylem and stem placed between two parallel plates were calculated as follows:

$$E = \frac{0.338k^{3/2}F\left(1-\mu^2\right)}{x^{3/2}}\left[\frac{1}{R'}+\frac{1}{R_1'}\right]^{\frac{1}{2}}, \quad (9)$$

where: k is a coefficient that depends on the geometrical characteristics of cotton stalks, $k = 1.303$, F is the compressive force (N), x is the deformation of the samples (m), μ is the Poisson's ratio, R' and R_1' are the small and large radii of curvature of the convex surface of the samples in contact with a flat surface (m), respectively (Fig. 4).

The thickness H of the samples was measured using a Vernier calliper. Eqs (10) and (11) were used to approximate R' and R_1':

$$R_1 \approx H/2, \quad (10)$$

$$R_1' \approx \frac{H^2+\frac{L^2}{4}}{2H}, \quad (11)$$

where: L is the length of the sample (m).

The force at the rupture point is the minimum force that the cotton stalk samples must be subjected to in order to crack (rupture). The values of force and deformation at the bio-yield and rupture points were directly measured from the force-deformation curve and recorded by the device used for the compression test. The energy absorbed by the samples until the rupture point is the energy required to break (rupture) the samples. The energy absorbed by the bio-yield and rupture points may be determined using the area under the force-deformation curve between the initial and bio-yield and rupture points, respectively, as follows:

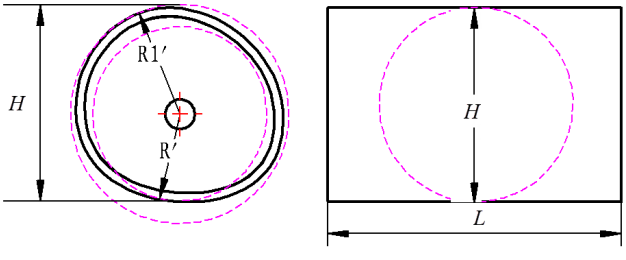

Fig. 4. Approximation of R_1 and R_1' for convex bodies.

$$RE = \int_0^x F(x)dx, \quad (12)$$

where: RE is the absorbed energy (J), F is the force at the rupture point (N), and x is the deformation at the rupture point (m).

The xylem and cotton stalk were cut into samples with lengths of 120 mm each and tubular cross-sections, where the external and inner diameters were the same as those of the original materials. The geometrical parameters (external and inner diameters) of various samples were measured. The support had a span L_s of 80 mm. A pretension force (<5 N) was applied on the samples at a loading velocity of 5 mm min^{-1} in a radial direction.

The mechanical properties of cotton stalks are closely related to their chemical constituents and microstructure. In the terms of chemical constituents, cellulose is the primary chemical constituent of a plant's cell wall, and is closely related to its material strength. Lignin constitutes a cellulose frame, which relates to the plant in a manner that is analogous to steel in concrete. The strength and stiffness of the plant material are mainly determined by lignin content. In order to assist in the analysis of the mechanical properties of cotton stalk, various standard methods were used (GBT 20805-2006, NYT 1459-2007, and GBT 20806-2006), and the contents of hemicellulose, cellulose and lignin in the cotton stalk and its tissues (phloem and xylem) were determined as referred to in Table 1 of the results section. A Fourier transform infrared spectrometer (ThermoFisher Nicolet iN10, USA.) was used to obtain the spectra of cotton stalk and its tissues in the transmitted light mode, as shown in Fig. 5. A scanning electron microscope (Zeiss Gemini 300, Germany) was used to obtain cross-sectional microscopic images of the cotton stalk and its tissues, as shown in Fig. 6.

RESULTS AND DISCUSSION

The results of the axial tensile test, radial compression test and bending test are shown in Tables 2-4, respectively. The mean and standard deviation values for E_{Z1}, E_{X1}, E_{Z2},

Table 1. Mass fractions of chemical constituents in each tissue of cotton stalk

Part	Content (%)			Total content (%)	Lignin/Cellulose (L/C)
	Hemicellulose	Cellulose	Lignin		
Phloem	12.15	38.75	19.62	70.52	0.51
Xylem	17.15	47.70	21.37	86.22	0.45
Stalk	9.43	48.18	20.31	77.92	0.42

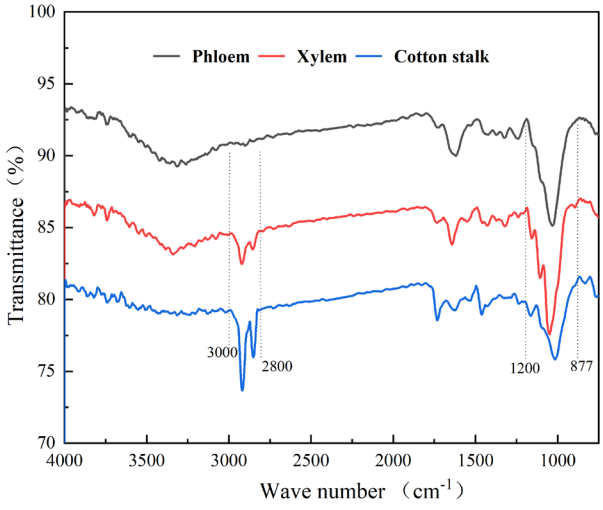

Fig. 5. FTIR of the cotton stalk and its tissues.

E_{X2}, E_{Z3} and E_{X3} are 3181.79±251.59 MPa, 91.04±7.99 MPa, 1093.91±64.49 MPa, 83.77±5.13 MPa, 249.89±19.29 MPa and 77.01±9.81 MPa, respectively. The mean and standard deviation values for G_{XZ2} and G_{XZ1} are 129.17±9.74MPa and 180.88±11.66 MPa. The calculated value of G_{XZ3} was obtained using Eq. (7) as 29.62 MPa. The following stalk xylem anisotropic-plane Poisson's ratios were obtained by substituting the results into Eq. (8): xylem $\mu_{YZ2} < 0.07$, phloem $\mu_{YZ3} < 0.398$, and cotton stalk $\mu_{YZ1} < 0.026$. Up to this point all elastic parameters concerning the cotton stalks and its tissues (xylem and phloem) have been determined based on the assumption of transverse anisotropic material properties, as shown in Table 4. By comparing the elastic modulus it was found that the cotton stalk showed significant differences in the axial and radial directions, and this difference was also present between the phloem and xylem. Using Eq. (4), $E_{X1\text{calculation}} = 80.89$ MPa was obtained, this value is relatively close to the tested value of E_{X1} 91.04 MPa, thereby indicating that the basic hypothesis of this study is valid, which is that the cotton culm is in fact a composite material with a cross-sectional anisotropy. This finding coincides with the FIRT and SEM results (see below for details). In addition, similar features were also found to be present in stalks such as sunflower and ramie (Kovács *et al*., 2019; Zhou *et al*., 2016; Liao *et al*., 2007). In the background of the composites theory, the results shown in Table 4 may be used to construct the constitutive equations for cotton stalks and to determine the equation coefficients. More information concerning the optimal method of constructing constitutive equations may be found in (Liu *et al*., 2007). The intrinsic constitutive equation for cotton stalk formed the basis of a numerical simulation and may be applied to a simulation study of cotton stalk uprooting and crushing implements, which was important for the optimal design of such implements.

As shown in Table 1, the total contents of hemicellulose, cellulose, and lignin in the phloem, xylem and cotton stalk were 70.52, 86.22, and 77.92%, respectively. The results showed that hemicellulose, cellulose, and lignin are the crucial constituents of the cotton stalk, with cellulose being the most abundant component. Cellulose is the primary chemical constituent of a plant's cell wall, and is

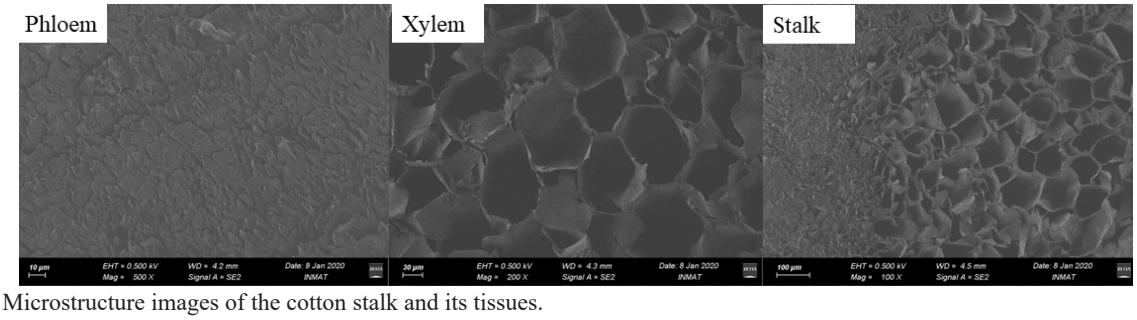

Fig. 6. Microstructure images of the cotton stalk and its tissues.

Table 2. Results of axial tensile tests

Part	D_e (mm)	T (mm)	CL (mm)	ME (MPa)	n
Stalk	7.09±0.57	4.52±0.28	10	3181.79±251.59(E_{Z1})	7[a]
	W (mm)	T (mm)	CL (mm)	ME (MPa)	
Xylem	6.88±0.30	3.84±0.32	10	1093.91±64.49 (E_{Z2})	9[b]
Phloem	4.24±0.24	0.76±0.05	10	249.89±19.29 (E_{Z3})	10

Date represents average values±standard deviation. D_e is equivalent diameter; T is thickness (mm); CL is calibration length (mm); ME is modulus of elasticity (MPa); W is width of sample; n is number of testing samples. [a] Three sample was damaged during testing and therefore was excluded. [b] One sample was damaged during testing and therefore was excluded.

Table 3. Results of radial compressive tests (n = 10)

L (mm)	H (mm)	R_1 (mm)	R_1' (mm)	ΔF (N)	x (mm)	ME (MPa)	RE (mJ)
				Xylem			
20.0±0.66	6.00±0.54	2.98±0.27	10.99±0.68	321.69±102.16	0.68±0.11	83.77±5.13 (E_{X2})	81±3.43
L (mm)	H (mm)	R_1 (mm)	R_1' (mm)	ΔF (N)	x (mm)	ME (MPa)	RE (mJ)
				Stalk			
20.0±0.53	7.00±0.49	3.46±0.25	10.31±0.37	378.40±98.51	0.74±0.11	91.04±7.99 (E_{X1})	84±4.64
				Phloem			
L (mm)	H (mm)	W (mm)	ΔF (N)		x (mm)	ME (MPa)	
20.0±0.81	0.80±0.05	16.14±0.73	13.75±8.02		0.14±0.03	77.01±9.81(E_{X3})	

Table 4. Results of radial bending tests (n = 10)

D_e	D_i	L_s	a	ΔF	f	f_1	U/N	G (MPa)
				(mm)				
					Xylem			
6.90±0.31	0.86±0.08	80	20	194.54±27.60	4.63±0.78	2.22±0.39	2376.12±498.41	129.17±9.74 (G_{XZ2})
					Stalk			
6.68±0.57	0.64±0.06	80	20	234.03±32.16	3.86±0.56	1.72±0.29	3095.41±786.13	180.88±11.66(G_{XZ1})

D_e is the external diameter, D_i is the inner diameter, L_s is the span, a is the extrapolation length, ΔF is the load increment of the elastic stage, f is the mid-span deflection increment, f_1 is the epitaxial deflection increment, U is the shear stiffness, and G is the bending shear modulus.

Table 5. Elastic parameters of each tissue of the cotton stalk

	E_X	E_Y	E_Z	G_{XY}	G_{XZ}	G_{YZ}	μ_{XY}	μ_{XZ}	μ_{YZ}
				(MPa)					
Stalk	91.04	91.04	3181.79	28.45	180.88	180.88	0.6	＜0.026	＜0.026
Xylem	83.77	83.77	1093.91	26.18	129.17	129.17	0.6	＜0.07	＜0.07
Phloem	77.01	77.01	249.89	29.62	248.85	248.85	0.3	＜0.398	＜0.398

E_X is the radial (X) elasticity modulus, E_Y is the radial (Y) elasticity modulus, E_Z is the axial elasticity modulus, G_{XY} is the axial torsional shear modulus, G_{XZ} is the radial (Y) bending shear modulus, G_{YZ} is the radial (Y) bending shear modulus, μ_{XY} is the Poisson's ratio (plane XY), μ_{XZ} is the Poisson's ratio (plane XZ), μ_{YZ} is the Poisson's ratio (plane YZ).

closely related to its material strength. Lignin constitutes the cellulose frame, which relates to plant stalk strength in a way that is analogous to the way that steel reinforcement relates to the strength of concrete. The strength and stiffness of the material are mainly determined by lignin content. Amorphous hemicellulose penetrates the matrix and acts as a bonding matrix enhancing the overall strength of the fibre (Aminian *et al*., 2006; Guo *et al*., 2009). As shown in Fig. 5, the transmittance of the three specimens of phloem, xylem and their combined cotton stalk were generally consistent, with the difference being in the intensity of the absorption peaks. This feature was consistent with the results shown in Table 1, *i.e*., the main components of the xylem, phloem and cotton stalk consisted of lignin, cellulose and hemicellulose, but the contents were slightly different. The absorption peaks at 1000 to 1100 cm^{-1} were characteristic peaks of cellulose and hemicellulose, for the most part they were generated by a C-O (C-O-C) stretching vibration and in the O-H plane, a bending vibration in the sugar unit. At 2800-3000 cm^{-1}, the characteristic absorption peaks were evident in the xylem and cotton stalk, but not in the phloem. Overall, the xylem and stalk had the closest transmittance curves. Small structural voids were found in the phloem, as seen in Fig. 6. A distinct, regular void structure, resembling a "honeycomb" structure was visible in the xylem. The cotton stalk had a dense and flexible skin structure. The internal structural form had a favourable stability and rigid support. The cotton stalk may be considered as a composite structure in cross-section.

A comparison analysis showed that the tensile elastic modulus E_Z was significantly higher than the compressive elastic modulus E_X, and also, the E_Z of the cotton stalk was

about 34 times higher than the E_X. This means that the axial stiffness of the cotton stalks is much higher than the radial stiffness. According to this mechanical property, it is suggested that the design of the cotton stalk uprooting device should be guided mainly by axial tensile lifting, and the friction force should be increased by improving the friction coefficient of the clamping mechanism, rather than increasing the radial clamping force to an excessive degree.

The tensile results showed that the tensile modulus of xylem E_{Z2} was about 4 times that of phloem E_{Z3}, and that stalk E_{Z1} was about 3 times that of xylem E_{Z2}. In addition, the tensile strength of the material is closely related to its cellulose content. Accordingly, a high cellulose content helps to increase the tensile strength (Zhao *et al.*, 2010). The cellulose contents of the stem, xylem, and phloem are 48.18, 47.7, and 38.75%, respectively (Table 5). Therefore, cotton stalk has the highest elastic modulus, followed by xylem (marginally lower), with phloem having the lowest elastic modulus.

Figure 7 demonstrates the force-deformation curves of the cotton stalk and its tissues. The *F-x* curves of the cotton stalk underwent distinct phase changes. The curve clearly highlights the bio-yield and rupture points. In the cotton stalk stretching process, the rupture point of the xylem appeared first, with no significant change in the phloem. The reason for this phenomenon might be related to the different elastic modulus between xylem and phloem. The reason for the difference in elastic modulus between the two may be related to their chemical composition. In general terms, the higher the lignin to cellulose (L/C) ratio, the tougher the material. The L/C ratios of phloem and xylem were found to be 0.51 and 0.45, respectively. Therefore, the phloem is tougher than the xylem. The xylem and phloem form a bond at the interface between the two, which results in a cotton stalk with composite properties. It should be noted that the bonding force at the contact interface was found to be limited and that the breakdown of the bond caused PPSAX. It was this characteristic that was exploited by the cotton stalk peeling machine to achieve the separation between xylem and phloem. The weak bonding force may be related to the hemicellulose content, as hemicellulose has the benefit of enhancing the strength of the tissue bonds, but the hemicellulose content (9.43%) in the cotton stalk was found to be lower than that in both the xylem (12.15%) and phloem (17.15%). It should be noted that a necessary prerequisite for PPSAX to arise was the phloem breaking in a radial direction. Therefore, there are two considerations that need to be taken care of in the design of the clamper, either the phloem should not be destroyed or the clamper should be properly embedded in the xylem.

The cotton stalk E_{X1} (91.04 MPa), xylem E_{X2} (83.77 MPa) and phloem E_{X3} (77.01 MPa) share a similar modulus of elasticity. The cotton stalk (84 mJ) and xylem (81 mJ) possess a similar rupture energy. The results show that in the radial direction, the compressive strength of cotton stalk is mainly determined by xylem. This may be related to the better flexibility and the lower thickness of the phloem. The modulus of elasticity of the cotton stalk and its tissues differed greatly in the axial and radial directions, and the main reasons for these differences may be related to factors such as the alignment direction and the closeness of the fibres.

As shown in Fig. 8, the xylem and stalk showed similar *F-x* curves; as the samples continued to deform, the force increased up to the first peak, decreased briefly and then increased up to the second peak, then plummeted to form a trough, and finally continued to increase. The entire variation trend may be divided into three stages: elastic deformation, plastic deformation, and rupture. Meanwhile, it was found that both the xylem and cotton stalk exhibited distinct bio-yield and rupture points. The phloem showed no obvious fracture points and no obvious damage due to compression. The reasons for this have been analysed with

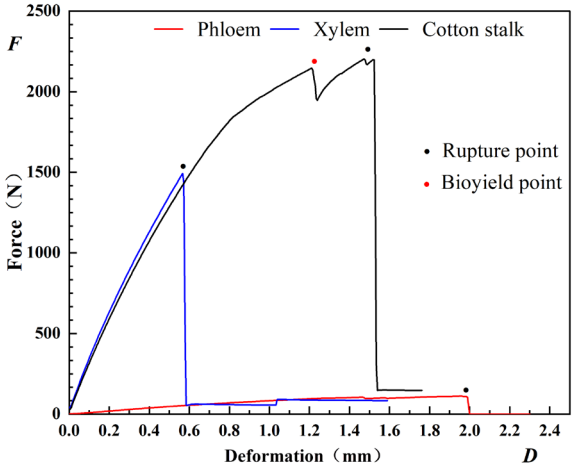

Fig. 7. Typical tensile force–deformation curves of the phloem, xylem, and stalk.

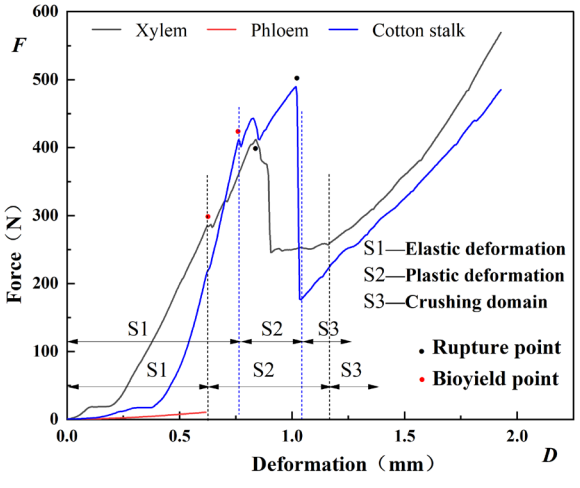

Fig. 8. Typical compression force-deformation curves of xylem, phloem, and stalk.

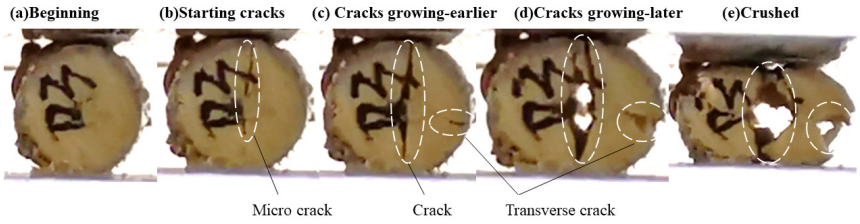

Fig. 9. Major breaking phenomenon at the internodal sections during compression.

regard to two aspects. The first was that the phloem is dense (Fig. 5a) and flexible, the second is that the samples were in the shape of a flat sheet, which may have some influence over the test results. According to the structural model characteristics of the cotton stalk material in Fig. 2, and also the compression process, five major phenomena were observed. At the beginning of the compression process, the sample did not incur any observable damage or breakage in its structure, this was due to its high lignin content (Fig. 9a). Subsequently, a straight vertical break occurred in the core of the sample in relation to one significant initial breaking phase (Fig. 9b). As the vertical breakage enlarged, the sample was ovalized, and the stress was transferred to the outer phloem. Small cracks appeared in the horizontal direction (Fig. 9c). The vertical and horizontal cracks continued to grow and expand (Fig. 9d) until the sample was completely crushed (Fig. 9e). The xylem had a great effect on the radial compressive behaviour of the cotton stalk. Notably, the phloem ruptured in the horizontal direction, but it did not incur any significant damage in the vertical direction.

The results of the compression tests show that the radial compressive strength of cotton stalk is obviously lower than the axial tensile strength, and that the compressive strength was mainly carried by the xylem network. Therefore, it may be assumed that the clamping force of the stalk puller exceeds the radial compression breaking force as a direct cause of FCS. Determining a reasonable clamping force is one of the most important measures required to reduce stalk breakage, but determining this value accurately could be quite challenging. The factors involved include the fact that even for stalks from the same area, the compression rupture force varies greatly due to differences in stalk diameter. It is almost impossible to use the same clamping force to ensure that the stalks are both successfully uprooted and do not fracture at the same time. The force applied should be based on a large number of tests and also the use of statistical principles to identify the optimal value of the clamping force. On this basis, increasing the uprooting force may be achieved by increasing the friction coefficient, the contact area and optimizing the clamping materials of the clamping mechanism. The application of such methods would help to reduce the stalk breakage and increase the uprooting success rate.

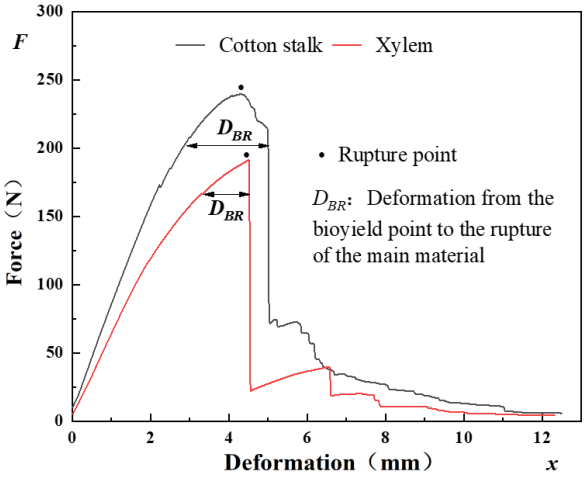

Fig. 10. Typical bending force-deformation curve.

According to the radial bending results, the xylem had an average bending shear modulus G_{XZ2} of 129.17 MPa, the cotton stalk had an average bending shear modulus G_{XZ1} of 180.88 MPa. An analysis of the bending shear modulus of the cotton stalk (G_{XZ1} of 180.88 MPa) and xylem (G_{XZ2} of 129.17 MPa) shows that 71.4% of the bending strength of the cotton stalk was supported by xylem, and 28.6% of the bending strength of the cotton stalk was supported by phloem.

Figure 10 illustrates the typical F-x curve of each component in the cotton stalk bending test. The xylem and cotton stalk have similar curves. Moreover, both samples resembled brittle materials. The cotton stalk had a bending force of 234.03 N at the rupture point, and a bending shear modulus of 180.88 MPa. The xylem had a bending force of 194.54 N at the rupture point, and a bending shear modulus of 129.17 MPa. The cotton stalk had a 28.59% greater bending shear modulus than the xylem.

In addition, the bio-yield point for the deformation D_{BR} of the main material rupture revealed that the stalk incurred a significantly greater degree of bending damage D_{BR} than the xylem, this was mainly due to the outer phloem. In other words, in the bending test, the bottom material of the sample cross section produced a tensile effect, and the cotton stalk sample had one more layer of phloem than the xylem sample. More importantly, the axially distributed fibres in

the phloem had a favourable tensile strength, and the xylem was destroyed after the phloem. Therefore, the stem had a higher bending shear modulus than the xylem.

When the specimen was subjected to a three-point bending force, the cotton stalk would have failed if the deformation deflection had exceeded 5 mm. Overall, the cotton stalk was found to have the characteristics of a brittle material; that is, it had weak flexural and shear resistances. The radial shear damage to the cotton stalk inflicted by the clamping mechanism during uprooting and the impact of the forward motion of the puller, which cause the stalk to bend, are the primary factors that caused the stalk to break.

CONCLUSIONS

1. A mechanical model of the cotton stalk was constructed based on the mechanics of composite materials. A theoretical model of the cotton stalk composite material was established through both experimental results and theoretical calculations, which shows that the cotton stalk has the characteristics of composite materials in the radial direction. The axis elasticity moduli of cotton stalk, xylem and phloem are 3181.79, 1093.91, and 249.89 MPa, respectively, whereas the radial elasticity moduli of these materials are 91.04, 83.77, and 77.01 MPa, respectively.

2. The reasons for fractured cotton stalk and peeled phloem sliding along the xylem were analysed from the point of view of the cotton stalk being a composite material. The cause of peeled phloem sliding along the xylem was mainly related to the different toughness of the xylem and phloem, as well as the weak cohesion between xylem and phloem. The xylem network is the backbone of the cotton stalk, it provides 96% of the compressive strength in the radial direction, an excessive radial load was found to be the direct cause of fractured cotton stalk. In addition, the entire cotton stalk was found to have the characteristics of a brittle material, and would be broken if the deformation deflection had exceeded 5 mm throughout the whole three-point bending process. Based on the results obtained, it is considered that the key to the design of the uprooting mechanism is to impose firm constraints within the radial compressive limit of the cotton stalk. In addition, avoiding or decreasing the radial shear and bending effect of the uprooting mechanism on the cotton stalk could also be effective.

Conflict of interest: The authors declare that they have no conflict of interest.

Compliance with ethical requirements: This study does not include any experiment involving human or animal subjects.

REFERENCES

American Society of Agricultural Engineers, **2017.** Compression test of food materials of convex shape.

Aminian F., Suarez E.D., Aminian M., and Walz D.T., 2006. Forecasting economic data with neural networks. Computational Economics, 28(1), 71-88. DOI:10.1007/s10614-006-9041-7.

Aydın İ. and Arslan S., 2018. Mechanical properties of cotton shoots for topping. Industrial Crops and Products, 112, 396-401. DOI:10.1016/j.indcrop.2017.12.036.

Cai J., Zhang J., Yeerbolati·T., and Gao Z., 2020. Design and Test of Clamping Belt Cotton Straw Harvester. Trans. Chinese Soc. Agric. Machinery, 51(10), 152-160. DOI:10. 6041/ j. issn. 1000-1298. 2020. 10. 017.

Chen M., Zhao W., Wang Z., and Zhang J., 2019a. Research status of the cotton-stalk uprooting technology. J. Chinese Agric. Mechanization, 40(05), 29-35. DOI:10.13733/j. jcam.issn.2095-5553.2019.05.06.

Chen M., Zhao W., Wang Z., and Liu K., 2019b. Operation process analysis and parameter optimization of dentate disc cotton-stalk uprooting mechanism. Trans. Chinese Soc. Agric. Machinery, 50(03), 109-120.

Chen M., Wang Z., Qu H., and Chen Y., 2015. Bending and tensile properties tests of the cotton-stalk. J. Chinese Agric. Mechanization, 36(05), 29-32.

Chen X., Liu H., Xia N., and Shang J., 2015. Preparation and properties of oriented cotton stalk board with konjac glucomannan-chitosan-polyvinyl alcohol blend adhesive. Bioresources, 10(2), 3736-3748. DOI:10.15376/biores.10.2.3736-3748.

Guo W., Wang F., Huang G., and Zhang F., 2009. Experiment on Mechanical Properties and Chemical Compositions of Wheat Stems. Trans. Chinese Soc. Agric. Machinery, 40(02), 110-114.

He X., Liu J., Wang X., and Xu Y., 2020.Design and Experiment of Row-controlled Shoveling and Drawing Placement Machine for Cotton-stalks Based on Agronomy of Close Planting. rans. Chinese Soc. Agric. Machinery, 51(10), 142-151. DOI:10. 6041/ j. issn. 1000-1298. 2020. 10. 016.

Hou X., Sun F., Zhang L., and Luo J., 2014. Chemical-free extraction of cotton stalk bark fibers by steam flash explosion. Bioresources, 9(4), 6950-6967. DOI:10.15376/biores.9.4.6950-6967.

Hu Z. and Nie X., 2014. Alkaline peroxide extrusion pulping of cotton bast and cotton stalk. Bioresources, 9(2), 2856-2865. DOI:10.15376/biores.9.2.2856-2865.

Jha S.K., Singh A., and Kumar A., 2008. Physical characteristics of compressed cotton stalks. Biosystems Eng., 99(2), 205-210. DOI:10.1016/j.biosystemseng.2007.09.020.

Kovács Á., and Kerényi G., 2019. Physical characteristics and mechanical behavior of maize stalks for machine development. Int. Agrophys., 33(4), 427-436. DOI:10.31545/ intagr/113335.

Li T., Hao F., Han Z., and Fang X., 2018.Theoretical analysis and experiment of picking cotton with horizontal spindle. rans. Chinese Soc. Agric. Machinery, 49(S1), 233-238. DOI:10. 6041/j.issn.1000-1298.2018.S0.031.

Li Y., Du X., Song Z., and Li F., 2011. Test of shear mechanical properties of cotton stalks. rans. Chinese Soc. Agric. Machinery, 27(02), 124-128.

Liang R., Chen X., Zhang B., and Peng X., 2020. Tests and analyses on mechanical characteristics of dwarf-dense-early major cotton variety stalks. Int. Agrophys., 34(3), 333-342. DOI:10.31545/intagr/122575.

Liao Y., Liao Q., Tian B., and Shu C., 2007. Experimental research on the mechanical physical parameters of bottom stalk of the *Arundo donax* L. in harvesting period. Trans. CSAE, (04), 124-129.

Liu Q., Ou Y., Wang W., and Qing S., 2007. The mechanical properties and constitutive equations of sugarcane stalk: 2007 ASABE Annual International Meeting, Minneapolis, Minnesota, ASABE.

Ramadan Y. Y. R., 2010. Development and evaluation of a cotton stalks puller. J. Soil Sci. and Agric. Eng., Mansoura Univ., 1(10), 1061-1073.

Shen C., Li X., Tian K., and Zhang B., 2015. Experimental analysis on mechanical model of ramie stalk. Trans. Chinese Soc. Agric. Eng. (Transactions of the CSAE), 31(20), 26-33. DOI:10.11975/j.issn.1002-6819.2015.20.004.

Shi N., Guo K., Fan Y., and Liu B., 2017. Peeling and shearing mechanical performance test of cotton stalks in extrusion state. Trans. Chinese Soc. Agric. Eng. (Transactions of the CSAE), 33(18), 51-58. DOI:10.11975/j.issn.1002-6819.2017.18.007.

Tan C., Li H., Wei D., and Lorenzo R., 2020. Mechanical performance of parallel bamboo strand lumber columns under axial compression: experimental and numerical investigation. Construction and Building Materials, 231, 117168. DOI:10.1016/j.conbuildmat.2019.117168.

Tang Z., Han Z., Gan B., and Bao C., 2010. Design and experiment on cotton stalk pulling head with regardless of row. Trans. Chinese Soc. Agric. Machinery, 41(10), 80-85.

Wang G., Zhang X., Gao Z., and Wang Y., 2017. Dynamic testing and analysis of Poisson's ratio constants of timber. Mechanics and Architectural Design, 18(9), 1-10. DOI:org/10.1142/9789813149021_0002.

Wu J. and Chen X., 2015. Present situation, problems and countermeasures of cotton production mechanization development in Xinjiang Production and Construction Corps. Trans. Chinese Soc. Agric. Eng., 31(18), 5-10.

Zhang G., Li Y., Li Z., and Zhang Y., 2014. Measuring system of cotton stalk real-time pull force in the field based on labview: 2014 ASABE and CSBE/SCGAB Annual Int. Meeting, Montreal, July 13-16, Quebec, Canada.

Zhang J., Gao Z., Cai J., and Tiemuer Y., 2021. Design and experiments of cotton stalk pulling machine with horizontal-counter rollers. Trans. Chinese Soc. Agric. Eng., 37(07), 43-52. DOI:10.11975/j.issn.1002-6819.2021.07.006.

Zhao C., Han Z., Cao Z., and Shi S., 2010.Stems Biomechanical Properties Experiment of Creeping Tangled Forage in Harvesting Period. Trans. Chinese Soc. Agric. Machinery, 41(6), 65-69, 92. DOI:10.3969/j.issn.1000-1298.2010.06.013.

Zhao W., Wang Z., Chen M., and Chen Y., 2019. Testing and parameter optimization of dentate disc multi-row cotton stalk uprooting device. Int. Agric. Eng. J., 28(4), 20-30.

Zhou Y., Li X., Shen C., and Tian K., 2016. Experimental analysis on mechanical model of industrial hemp stalk. Trans. Chinese Soc. Agric. Eng., 32(9), 22-29.